

Production and characterization of encapsulated Thymoquinone loaded bacterial cellulose/chitosan composite nano film and investigation of its in vitro antibacterial activity

Follow this and additional works at: <https://www.jfda-online.com/journal>



Part of the [Food Science Commons](#), [Medicinal Chemistry and Pharmaceutics Commons](#), [Pharmacology Commons](#), and the [Toxicology Commons](#)



This work is licensed under a [Creative Commons Attribution-NonCommercial-No Derivative Works 4.0 License](#).


Recommended Citation

Bayraktar, Aytul and Tuba, Tunc (2024) "Production and characterization of encapsulated Thymoquinone loaded bacterial cellulose/chitosan composite nano film and investigation of its in vitro antibacterial activity," *Journal of Food and Drug Analysis*: Vol. 32 : Iss. 3 , Article 6.

Available at: <https://doi.org/10.38212/2224-6614.3516>

This Original Article is brought to you for free and open access by Journal of Food and Drug Analysis. It has been accepted for inclusion in Journal of Food and Drug Analysis by an authorized editor of Journal of Food and Drug Analysis.

Production and characterization of encapsulated Thymoquinone loaded bacterial cellulose/chitosan composite nano film and investigation of its *in vitro* antibacterial activity

Aytul Bayraktar ^{a,*} , Tuba Tunç ^b

^a Department of Chemical/Bioengineering, Suleyman Demirel University, Isparta 32260, Turkey

^b Department of Bioengineering, Suleyman Demirel University, Isparta 32260, Turkey

Abstract

In this study, nanostructured thin films were produced from thymoquinone (TQ)-loaded composites encapsulated with different ratios of bacterial nanocellulose (BNC) to chitosan (CS). The study aimed to investigate their characterization, antibacterial effects, and potential as drug film coating materials. Chemical features and morphological characteristics were determined, and release tests and antibacterial assays were conducted on the thin film layers. As a result, BNC/CS-thymoquinone composite films obtained at different ratios were found to exhibit the highest antibacterial effect, particularly films with a 70% BNC/CS to 30% thymoquinone ratio, against *Salmonella typhimurium* bacteria.

Keywords: Bacterial nano-cellulose, Chitosan, Drug film coating, Thin film, Thymoquinone

1. Introduction

Today, biodegradability, biocompatibility, and the availability of natural materials for use as drug delivery tools are increasingly important [1]. In both the pharmaceutical industry and recent studies, drug delivery systems are commonly utilizing materials such as cellulose, chitosan, starch, alginate, carrageenan, and hyaluronic acid due to their exceptional properties. These biopolymers are chosen for drug encapsulation, transport within the body, and controlled release systems because of their ability to be readily absorbed and rapidly excreted after drug administration [2].

Thin film coatings used in drug release serve multiple purposes: they preserve the basic material integrity of tablets against environmental factors, mask their flavor, regulate drug release, and reduce potential damage during mechanical handling, creating a rigid, high-quality structure [3]. These thin films, whether with or without plasticizer polymeric matrices, are thin and flexible, meeting various

requirements for efficient use as a drug delivery platform [4]. An ideal film layer should possess desirable properties, including sufficient drug loading capacity, a fast dissolution rate or prolonged shelf-life, acceptable formulation stability, and non-toxic, biocompatible, and degradable characteristics [5,6]. Such films offer numerous advantages, such as increased bioavailability, enhanced patient compliance, ease of transport during production and shipping, and cost-effectiveness in formulation development, compared to conventional dosage forms [7,8]. Furthermore, thin films are less fragile and easier to dispense than orally disintegrating tablets, which necessitate special packaging [9,10].

Firstly, it is desirable that the types of polymers used in drug delivery applications are non-toxic, non-carcinogenic, non-allergenic, highly purified, reproducible, and have a well-defined release profile and *in vivo* degradation, ultimately being degraded in the body [11]. Bacterial cellulose and chitosan possess these properties, making them ideal biopolymers for drug delivery applications.

Received 20 October 2023; accepted 3 June 2024.
Available online 13 September 2024

* Corresponding author at: Suleyman Demirel University, Department of Chemical Engineering, Cunur/Isparta 32260, Turkey.
E-mail address: aytulbayraktar@sdu.edu.tr (A. Bayraktar).

<https://doi.org/10.38212/2224-6614.3516>

2224-6614/© 2024 Taiwan Food and Drug Administration. This is an open access article under the CC-BY-NC-ND license (<http://creativecommons.org/licenses/by-nc-nd/4.0/>).

Chitosan demonstrates excellent film-forming abilities due to its wound healing, antibacterial activity, responsiveness, biodegradability, biocompatibility, and non-toxicity, making it widely utilized in medicine and the biomedical field [12]. Derived and purified from natural biological sources, chitosan has found applications in wound dressings, sutures, and tissue engineering scaffolds owing to its biocompatibility and non-toxicity [13–15]. Moreover, chitosan has been extensively researched for its potential in developing drug delivery systems, benefiting from its favorable biodegradability *in vivo* [16]. However, chitosan films tend to have low elasticity and are thin and fragile [17].

In contrast to chitosan's fragility, bacterial cellulose (BNC), a natural cellulose polymer synthesized by certain microorganisms, possesses a highly hydrophilic structure, elasticity, biocompatibility, high purity, and superior mechanical properties [18]. With its reticulated structure, BNC exhibits excellent water absorption and capacity, rendering it a suitable candidate for film coating [19–21]. Furthermore, the special nanofibril structure of BNC makes it an ideal macromolecular support for the development of controlled release systems when combined with drugs [22].

Thymoquinone (TQ; 2-isopropyl-5-methyl-1,2-benzoquinone) is recognized as an active component in *Nigella sativa* seeds [23]. Extensive research has demonstrated that TQ exhibits various pharmacological activities, including antioxidant, anti-inflammatory, cardioprotective, hepatoprotective, antidiabetic, neuroprotective, and anticancer properties. TQ is known to exert its biological effects by modulating physiological and biochemical processes involved in reactive oxygen species (ROS) generation. In normal tissues, TQ acts as a potent antioxidant, inhibiting tumour cell proliferation through the suppression of superoxide radicals and lipid peroxidation, while enhancing the activities of antioxidant enzymes such as glutathione transferase, superoxide dismutase, catalase, and reductases [24]. Consequently, TQ offers therapeutic benefits against treatment-resistant advanced tumour cells by targeting molecular determinants crucial for cancer cell survival and progression [24,25].

The aim of this review is to provide a summary of the most recent literature on the use of TQ for the prevention and treatment of various diseases, along with possible mechanisms of action, and its potential use as a complementary or alternative medicine. In essence, TQ holds promise as a novel drug candidate for clinical trials. Interestingly, liposome- or nanoparticle-based formulations of TQ have

demonstrated enhanced efficacy against various diseases in animal models. Therefore, understanding the molecular mechanisms underlying TQ's action may pave the way for the development of therapeutic formulations to treat a wide range of diseases.

In this preliminary study, BC/Ch was chosen for its inherent nanostructures, high surface area, ultralightweight properties, non-immunogenic nature, and excellent chemical stability, making it an ideal candidate as a nanoparticle-mediated carrier. As a nanoscale drug delivery platform, BC/Ch allows for the chemical functionalization of its external surfaces with desired bioactive peptides [26], genes, or drugs, while its internal cavities can encapsulate bioactive molecules [27]. Moreover, these nanomaterials possess the capability to transport therapeutic molecules directly to targeted cell cytoplasm via a nanoneedle-like mechanism, without inducing cellular apoptosis [28].

For this investigation, we prepared and evaluated the drug delivery profiles of TQ-loaded BNC/Ch with four different biopolymer coating ratios. The prepared samples were designated as follows: 10% (BNC/Ch) - 90% TQ, 30% (BNC/Ch) - 70% TQ, 70% (BNC/Ch) - 30% TQ, and 90% (BNC/Ch) - 10% TQ. Given the widespread use of these coating materials in both research laboratories and the manufacturing industry, further experimental studies are warranted.

2. Materials and methods

In this study, bacterial cellulose was produced by *Lactobacillus rhamnosus* (DSM, DELVO-ADD 100R, Netherlands). Whey (PAS), sourced from Ünsüt (Isparta/TURKEY), served as the organic medium and was stored at +4 °C. Thymoquinone (TQ) (Sigma Aldrich 274666, USA) and Chitosan (Ch) (Mw = 50–190 kDa, degree of deacetylation: 75–85%, Sigma Aldrich 448969, Iceland) were used as materials in the study.

2.1. Production of bacterial nano-cellulose

In a study conducted by Cansu (2015), the most efficient BNC-producing bacterial culture condition for *L. rhamnosus* (DSM, DELVO-ADD 100R, Netherlands) was determined to be 75% whey (PAS) + 25% MRS medium + 10% activated culture at pH 5, resulting in a yield of 3.06 g. In our study, we applied the same optimal conditions for culturing the *L. rhamnosus* bacteria. For the pre-enrichment of *L. rhamnosus* bacteria, a bacterial stock culture was inoculated at 10% in MRS liquid medium and

cultured anaerobically for 24 h at 37 °C. Additionally, proteins were precipitated from PAS at 121 °C for 20 min with denaturation and removed by filtration. The bacterial cellulose production was allowed to incubate for 12 days at 28 °C in a medium consisting of 10% activated culture, 75% PAS +25% MRS, and pH 5, with a final volume of 100 mL in 34 × 19 cm glass beads. At the end of the 12-day incubation period, the produced BNC was separated by filtration and left to dry at 27 °C [29].

2.2. Film preparation of TQ in addition BNC/chitosan composite biopolymer

For the preparation of the TQ film, the optimal BNC/Ch ratio was determined based on the thesis studies of Cansu (2016) and Tuba (2018). The BNC/Ch solution was prepared by adding 1.5 g of chitosan, 0.2 g of Tween 80 (Fluka Chemie, Steinheim) as a surfactant, 0.5 g of glycerol as a plasticizer and cross-linker (AMRESCO, 0854, Solon, Ohio), and adjusting the volume to 100 mL with a 1% (v/v) lactic acid solution containing 1% lactic acid (Tekkim, 27081552, Turkey). In the preparation of the chitosan film, glycerin with lactic acid was used as a cross-linker and plasticizer, following a formulation modification proposed by Fajardo et al. (2010). The mixture was centrifuged for 4 h at 20 °C and stirred for 10 min at 5000 rpm in a magnetic stirrer. After removing the solids, 1 g of BNC was added to the remaining liquid and homogenized by stirring for 2 h. The BNC/Ch solution and TQ were then homogenized by mixing for 2 h in the volumes specified in Table 1, with a final volume of 20 mL. After the homogenization process, a thin film of approximately 0.30 mm thickness was spread onto 90 mm and 57 mm diameter petri dishes and allowed to dry for 16 h at 35 °C in the oven [30].

The composite film was characterized and subjected to antibacterial tests using chemical analysis and the shake flask method.

2.2.1. Analysis of OD (optical density)

The bacterial cell growth was monitored using a UV Spectrophotometer, which measures optical

density. UV Spectrophotometers operate in the visible region, where the optical density of photons is determined by absorption or emission as substances pass through the material. In our study, optical density was used as an indicator of bacterial growth progression.

2.2.2. Analysis of FTIR (Fourier transform infrared spectroscopy)

The FTIR Spectrum Analyzer is employed to identify organic compounds, as the IR spectrum of each compound, with the exception of optical isomers, is unique. This analysis occurs within the IR region of the electromagnetic spectrum, situated between the visible and microwave regions, with wavelengths ranging from 400 to 4500 cm⁻¹. In our study, FTIR analysis was conducted using a PerkinElmer BX IR spectrometer (PerkinElmer, Waltham, MA, USA) at the Laboratory of Experimental and Observational Student Research and Application Center of Suleyman Demirel University.

2.2.3. Analysis of FE-SEM (scanning electron microscopy)

Scanning electron microscopy was employed to analyze the surface structure of the samples obtained and dried after a 24-h incubation period at 37 °C. The microstructure was observed using a field emission scanning electron microscope (FE-SEM, HITACHI-S4800) at the Energy Research and Research Application Center of Suleyman Demirel University in Isparta.

2.2.4. Antibacterial test by shake flask method

The antibacterial test was conducted using the Shake flask method, a commonly employed quantitative technique that serves as a standard test for assessing the antimicrobial activity of agents. In this study, films containing 90% (BNC/CH) - 10% T and 70% (BNC/CH) - 30% T were tested against pathogenic strains of gram-positive and gram-negative bacteria, including *Escherichia coli* (ATCC 25922), *Staphylococcus aureus* (ATCC 6538), and *Salmonella typhimurium* (ATCC 14028).

Table 1. BNC/CH solution, Thymoquinone quantities in formed films.

	The amount of BNC/Ch solution (mL)	The amount of Thymoquinone (mL)	Dry weights (g)
%10(BNC/Ch)-%90 Thymoquinone	2	18	BS-Ch ratio is not enough for film formation
%30(BNC/Ch)-%70 Thymoquinone	6	14	0,12
%70(BNC/Ch)-%30 Thymoquinone	14	6	0,32
%90(BNC/Ch)-%10 Thymoquinone	18	2	0,47

The growth inhibition of bacteria was monitored over a 24-h period at 37 °C using an orbital shaker placed inside an incubator, with changes in optical absorbance recorded over time. Film samples weighing 0.45 g each were cut into small pieces and placed into test tubes containing 10 mL of nutrient broth. Subsequently, 0.225 µL of inoculated *E. coli*, *S. aureus*, and *Salmonella typhimurium* bacterial

logarithmic, and exponential equations. According to Lambert–Beer's law, concentration is directly proportional to absorption. Consequently, there is a direct proportionality between oscillation and absorption. Therefore, the percentage of oscillation at any time is proportional to the absorbance percentage at that time. Cumulatively, these percentage values are equal. From this perspective,

Cumulative oscillation rate at any time

$$= \frac{(\text{absorption value measured at that time} - \text{initial absorption value})}{\text{absorption value measured at that time}} \times 100$$

strains were added to each test tube.

Following inoculation, the test tubes were incubated for 24 h at 110 rpm in an orbital shaker incubator at 37 °C. After the incubation period, the absorbance values of the samples were measured using UV–Vis Spectroscopy. The antibacterial activities of the films were determined based on the measured absorbance values.

2.2.5. Measuring film thickness with callipers

The film thicknesses were measured using callipers, as thickness is a critical factor affecting their strength. Among the dry-weighted films, the highest yields were obtained with 90% (BNC/CH) - 10% TQ ratio, resulting in a yield of 0.47 g, and with 70% (BNC/CH) - 30% TQ ratio, yielding 0.32 g.

2.2.6. Release of TQe in addition BNC/Ch composite from film

The release test was conducted using the spectrophotometric method. Samples were prepared by cutting 12.5 mm² pieces of the TQ-added BNC/Ch composite film, which were then fully dissolved in 3.5 mL of PBS solution at pH 7.4 to mimic the alkaline systemic environment. Absorbance measurements were taken as kinetic scans at 257 nm for TQ release using an Agilent Technologies Cary 60 UV–Vis instrument. The results yielded an R² value of 0.8435 when analyzed mathematically. Based on the absorbance values, the cumulative drug release was evaluated as a percentage.

UV absorbance measurements were carried out directly without altering the sample or withdrawing solvent. To validate the mathematical feasibility of the graphs formed by the changing absorbance values over time for calculating cumulative oscillation, R² values were examined according to linear,

Calculated on this principle.

3. Results and discussion

The physical, characteristic and antibacterial properties of the biopolymer films obtained by mixing in a 24-h agitator were compared.

3.1. Results of FTIR analysis

FTIR analysis was conducted to characterize TQ-added BNC/Ch composites. Previous studies have reported that BNC and Ch exhibit good compatibility and miscibility due to their similar molecular structures [31,32]. The peaks obtained at 1647 cm⁻¹, 1575 cm⁻¹, and 1375 cm⁻¹ in the composite FTIR spectrum correspond to amide-I, amide-II, and amide-III, respectively. Similar results were observed in this study, with vibration bands at 1635 cm⁻¹, 1560 cm⁻¹, and 1404 cm⁻¹ in the FTIR spectrum. The peak at 3500 cm⁻¹ indicates the OH stretching vibration [31,33]. Previous studies have also investigated the preparation and characterization of BNC/Ch composites for potential biomedical applications, confirming the compatibility and miscibility of BNC and Ch. A wide band at 3450 cm⁻¹ in pure BNC corresponds to the OH stretching vibration. In the FTIR spectrum of the 90% (BNC/Ch) - 10% TQ composite, a strong vibration band at 3430 cm⁻¹ is observed, believed to result from a combination of the N–H stretching vibration and the O–H stretching vibration (Fig. 1).

The band at 2820 cm⁻¹ corresponds to the aliphatic CH group. Additionally, a sharp and distinct band at 1080 cm⁻¹ is observed due to COC stretching. In the BNC/Ch composite, the NH stretching vibration band is observed at 3420 cm⁻¹, overlapping with the OH stretching vibration band.

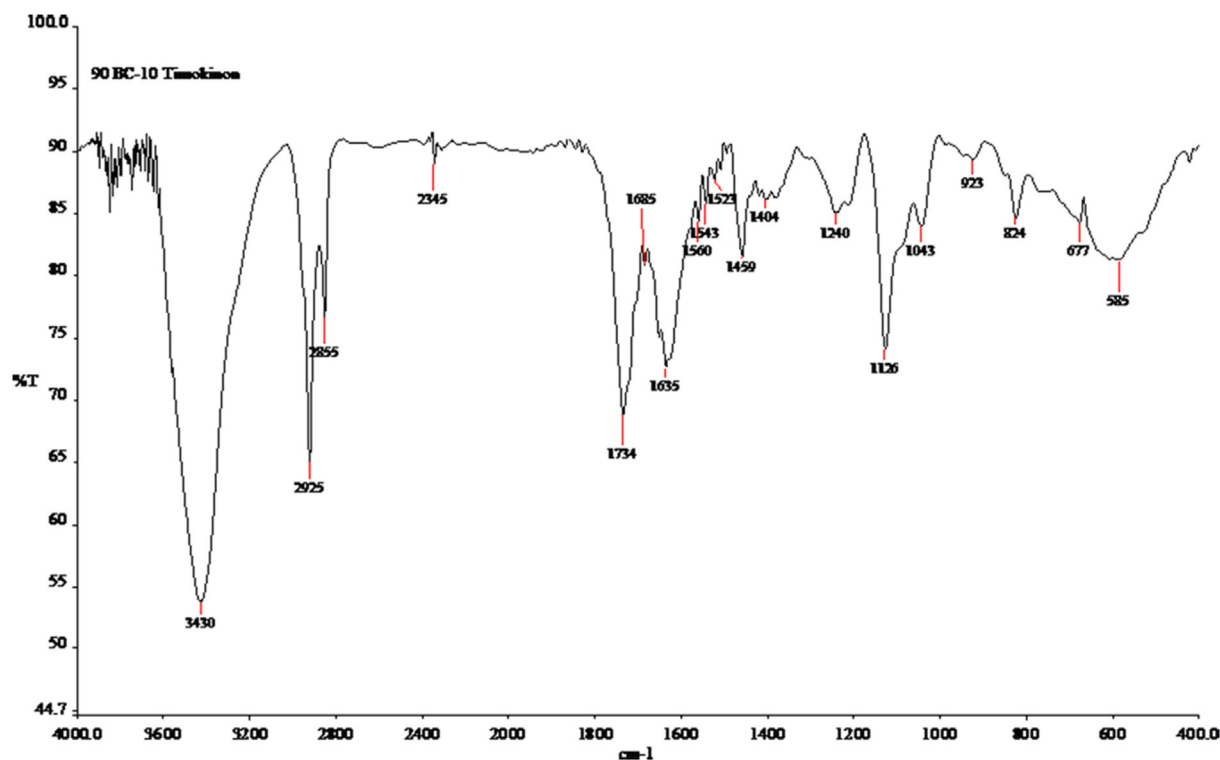


Fig. 1. FTIR spectrum of 90% (BNC + Ch) - 10% TQ composite.

The peaks observed at 1647 cm^{-1} , 1575 cm^{-1} , and 1375 cm^{-1} correspond to amide-I, amide-II, and amide-III, respectively, in the FTIR spectrum of the composite [31]. Similarly, vibration bands observed at 1635 cm^{-1} , 1560 cm^{-1} , and 1404 cm^{-1} in the FTIR spectrum of the 90% (BNC + Ch) - 10% TQ composite are believed to be associated with amide groups, albeit with a slight shift.

Fig. 2 displays the FTIR spectrum of the composite prepared with a ratio of 70% (BNC + Ch) - 30% TQ, indicating a decrease in the BNC ratio. The N–H vibration band was observed at 3429 cm^{-1} , while the vibration bands corresponding to amide-I and amide-III appeared at 1633 cm^{-1} and 1376 cm^{-1} , respectively. No amide-II band was observed.

Pagola S. et al. interpreted the results of FTIR analysis for TQ in their studies of the crystal structure of TQ [34]. They corresponded to the C–H stretching of dense band aliphatic groups at 2967 cm^{-1} , describing the characteristic strong stretching band of the carbonyl group of cyclohexadiene, which is interpreted as the result of FTIR analysis for TQ in their studies of the crystal structure of TQ. The characteristic strong stretching band of the carbonyl group, a cyclohexadiene, is observed at 1650 cm^{-1} wavelength, supported by reported values for TQ (1648 cm^{-1}) and 1,4-benzoquinone (1661 cm^{-1}). The weaker band observed at a higher wavelength ($\sim 3040 \text{ cm}^{-1}$), the strain

observed at C–H at C = C–H has been assigned. The dense band at 2967 cm^{-1} corresponds to C–H stretching of aliphatic groups. This property can be seen more clearly as an isolated band in the spectrum of 1,4-benzoquinone (without aliphatic C–H stretches) at 3058 cm^{-1} C = C stretching (1640–1675 cm^{-1}) gave an isolated and moderately strong band at 1440 cm^{-1} in 1,4-cyclohexadiene. The C = C stretching band cannot be precisely defined because the strong carboxy stretching band in the thymus is also present in this frequency range. It is also expected that the density of the C = C band is lower than that of both the carboxylic band and C = C stretching in 1,4-cyclohexadiene without cyclic and isopropyl substituents; it was noted that there was a transition at 1673 cm^{-1} (also present at 1,4-benzoquinone at 1678 cm^{-1}) slightly separated from the carbonic band and that it could be temporarily attributed to the C = C stretching band.

The stretching band of the carbonyl group, present in cyclohexadiene, observed in the FTIR sample of the 90% (BNC/Ch) - 10% TQ and 70% (BNC/Ch) - 30% TQ composites obtained in this study, is observed at 1635 cm^{-1} , respectively. It is hypothesized that some of the TQ may have evaporated during the analysis, which could be a reason why the peaks are not as strong. SEM images support this hypothesis (Fig. 3).

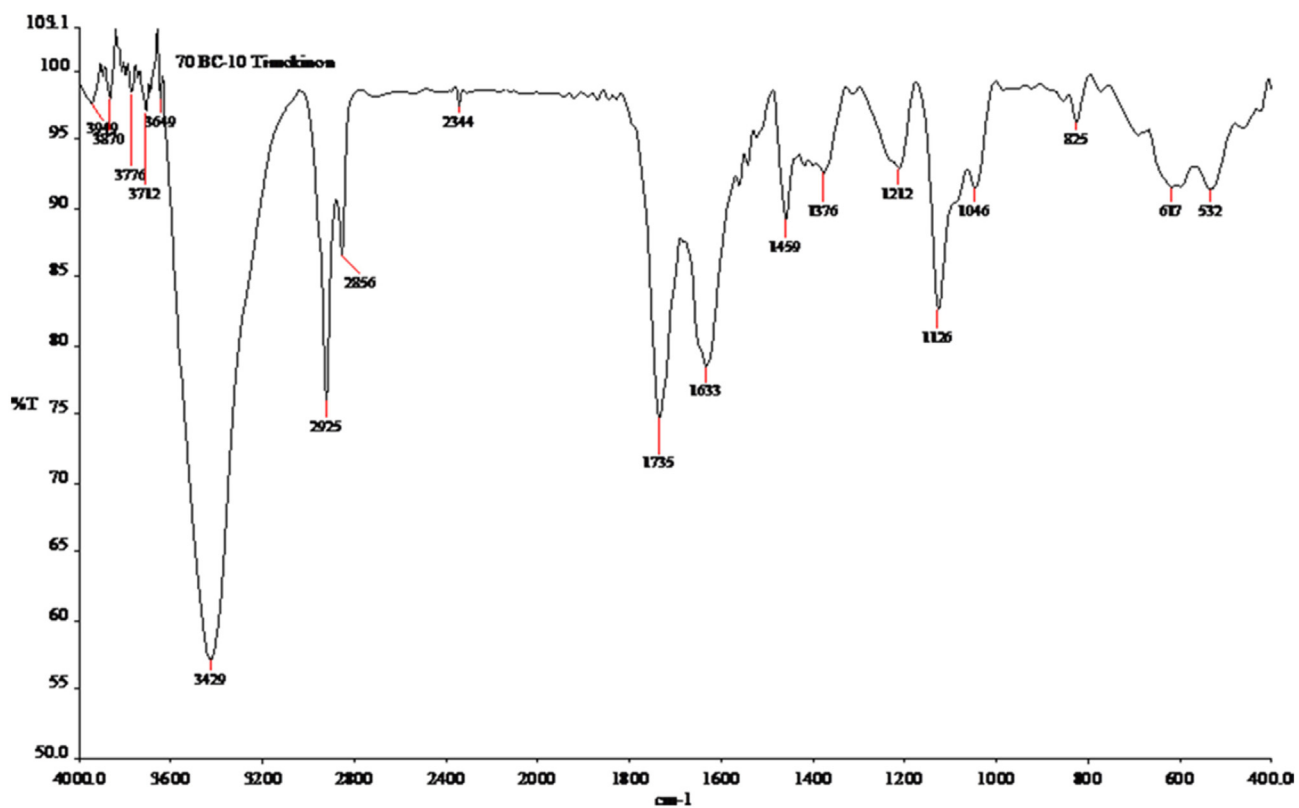


Fig. 2. FTIR spectrum of 70% (BNC + Ch) - 30% TQ composite.

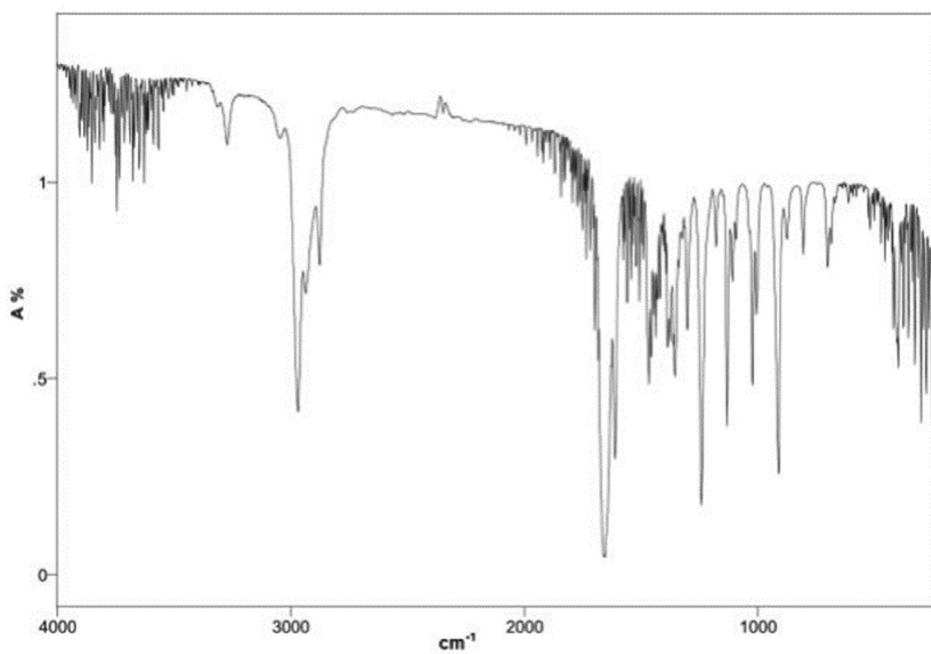


Fig. 3. FTIR spectrum of TQ.

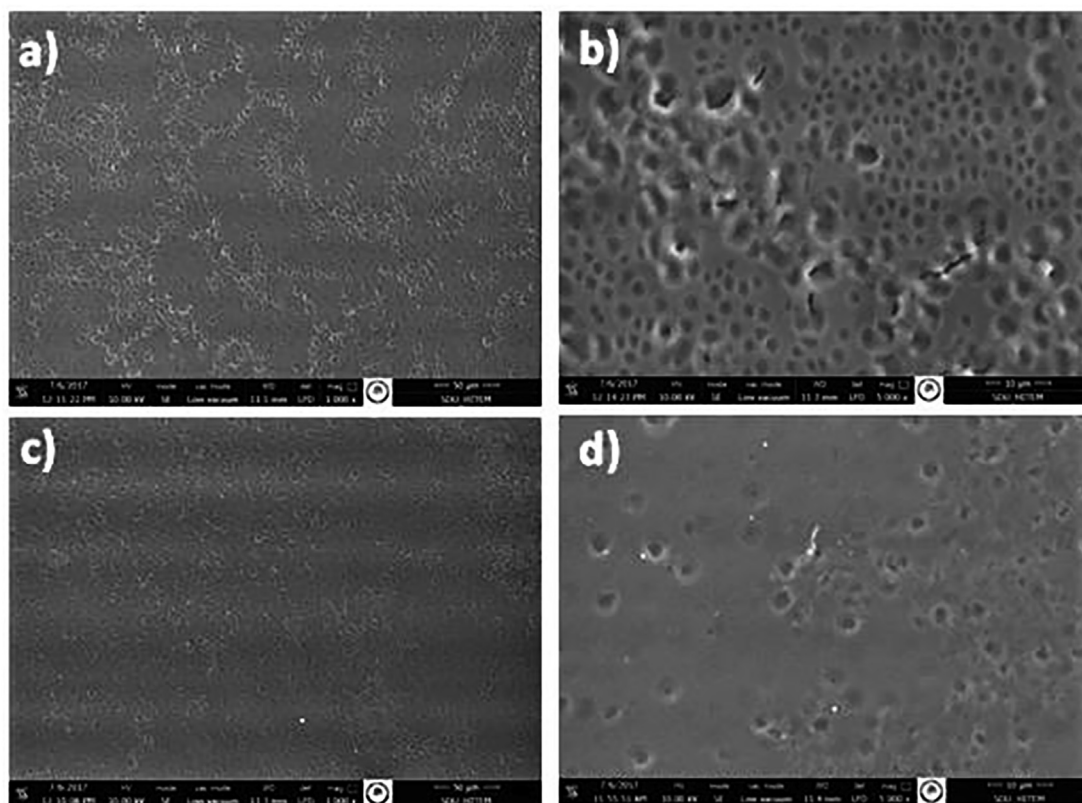


Fig. 4. SEM images of: a) %70 (BNC/Ch)-% 30 TQ film (10 μm), b) %70 (BNC/Ch)-% 30 TQ film (50 μm), c) %90 (BNC + Ch)-% 10 TQ film (10 μm), d) %90 (BNC + Ch)-% 10 TQ film (50 μm).

3.2. Results of SEM analysis

SEM images provide valuable insights into the morphological structure of nano-sized samples. In this study, sections of films containing 90% (BNC/Ch) - 10% TQ and 70% (BNC/Ch) - 30% TQ were examined under scanning electron microscopy. Fig. 4 displays SEM images of BNC, Ch, and TQ-loaded Ch composite nanoparticles at different concentrations with 70% (BNC + Ch) - 30% TQ and 90% (BNC + Ch) - 10% TQ ratios. The images reveal spherical particles with uniform morphology. Notably, an increase in the TQ ratio correlates with a higher number of globules observed in the SEM image. This finding is consistent with a study by Kucukozet O. A., titled "Production of edible films containing oleoresin and determination of some properties," where the SEM image of starch-sodium caseinate-based oleoresin-containing films exhibited a similar dispersion of oleoresin within the film layer, reminiscent of TQ [35]. Ostadhossein F. et al. examined SEM images of the composites in their study focused on developing BNC/Ch composite films incorporating nanomelias as a potential and flexible platform for wound dressing. Their findings

revealed that the blending of Ch with BNC led to a more densely packed BNC structure, as evidenced by the intensified fibrillary network [35]. Tong Sun et al. (2016) investigated the preparation and characterization of nano SiO_x-modified Ch coatings in their research titled "Preservation properties and preparation of synthesized nano SiO_x modified Ch coatings." They found that SiO_x had a significant impact on the micro morphology and microstructure of Ch coatings. Similarly, in another study, variations in the Ch and BNC ratio were observed to influence the characteristic and morphological properties of the produced film [36].

In this study, the composition of the BNC fibril webs within the BNC/Ch composite structure is not evident due to the presence of Ch. The SEM images illustrate TQ particles in spherical form, likely attributable to their specific surface area. Moreover, an increase in the TQ ratio correlates with a higher number of spherical forms, as depicted in the figures. Notably, SEM images captured at equal distances of 50 μm and 10 μm in Fig. 4 reveal a greater abundance of TQ particles in the coating of 70% (BNC/Ch) - 30% TQ compared to the 90% (BNC/Ch) - 10% example.

Table 2. Antibacterial test method.

Film layer ratios	Groups	Bacterial species	Amount of film layer (g)
%90 (BNC + Ch)-%10 Thymoquinone	C(Control)1	<i>Salmonella typhimurium</i>	–
	1	<i>Salmonella typhimurium</i>	0,45
%90 (BNC + Ch)-%10 Thymoquinone	C 2	<i>Escherichia coli</i>	–
	2	<i>Escherichia coli</i>	0,45
%90 (BNC + Ch)-%10 Thymoquinone	C 3	<i>Staphylococcus aureus</i>	–
	3	<i>Staphylococcus aureus</i>	0,45
%70 (BNC + Ch)-%30 Thymoquinone	C 4	<i>Salmonella typhimurium</i>	–
	4	<i>Salmonella typhimurium</i>	0,45
%70 (BNC + Ch)-%30 Thymoquinone	C 5	<i>Escherichia coli</i>	–
	5	<i>Escherichia coli</i>	0,45
%70 (BNC + Ch)-%30 Thymoquinone	C 6	<i>Staphylococcus Aureus</i>	–
	6	<i>Staphylococcus Aureus</i>	0,45

Furthermore, some dispersion was observed on the surface of TQ spheres in the SEM images of 70% (BNC/Ch) - 30% TQ samples. These dispersed particles are believed to stem from the volatility of TQ.

3.3. Antibacterial test results with shake flask method

The antibacterial test employed the Shake flask method, utilizing *E. coli*, *S. aureus*, and *Salmonella typhimurium* as pathogenic bacteria. Films containing 90% (BNC/Ch) - 10% TQ and 70% (BNC/Ch) - 30% TQ were subjected to this test. Both the agar diffusion method and the shake flask method were selected for the antibacterial test. The shake flask method was chosen because it simulates the conditions encountered in the stomach and intestine, where the drug-coated film is absorbed and undergoes disintegration. Equal amounts of bacteria, specifically 0.255 μ L, were utilized for each test, with Table 2 serving as the basis for test planning.

The media generated according to Table 3 were allowed to develop for 1 day at 37 °C and after one day optical density was measured on a UV spectrophotometer to determine the bacterial density and thus the values in Table 2 were obtained.

The highest proliferation was observed at a density of 0.806 abs in *Salmonella typhimurium* bacteria from the control group of films with a 90% (BNC/Ch) - 10% TQ ratio. The most significant difference between the control group and the samples was noted as 0.604 in the sample of *Salmonella typhimurium* bacteria for the 90% (BNC/Ch) - 10% TQ ratio. When examining the chart values, the antibacterial effect of the films varies depending on the type of bacteria. The most notable antibacterial effect on both sides of the film was observed in *Salmonella typhimurium*. Additionally, the antibacterial effects of films with a 70% (BNC/Ch) - 30% TQ ratio on *E. coli* and *S. aureus* were very similar and effective. This effect is notably higher compared to the effect of 90% (BNC/Ch) - 10% TQ on *E. coli* and *S. aureus*. It is evident that the rates of 70% (BNC/Ch) - 30% TQ are more effective in terms of antibacterial activity, which is likely related to the increased TQ ratio in the basal source. Halawani E. and Al-Jabre S. et al. reported that TQ exhibited antibacterial activity against *E. coli*, *Pseudomonas aeruginosa*, *Shigella flexneri*, *Salmonella typhimurium*, *Salmonella enteritidis*, and *Staphylococcus*.

In conclusion, BNC/Ch-TQ composite films obtained at different ratios exhibited the highest

Table 3. Optical density measurement result.

Film layer ratios	Groups	Bacterial species	Absorbance (abs)
%90(BNC/Ch)-%10 Thymoquinone	C (Control)1	<i>Salmonella typhimurium</i>	0,806
	1	<i>Salmonella typhimurium</i>	0,202
%90(BNC/Ch)-%10 Thymoquinone	C 2	<i>Escherichia coli</i>	0,675
	2	<i>Escherichia coli</i>	0,358
%90(BNC/Ch)-%10 Thymoquinone	C 3	<i>Staphylococcus aureus</i>	0,703
	3	<i>Staphylococcus aureus</i>	0,323
%70(BNC/Ch)-%30 Thymoquinone	C 4	<i>Salmonella typhimurium</i>	0,735
	4	<i>Salmonella typhimurium</i>	0,178
%70(BNC/Ch)-%30 Thymoquinone	C 5	<i>Escherichia coli</i>	0,750
	5	<i>Escherichia coli</i>	0,212
%70(BNC/Chitosan)-%30 Thymoquinone	C 6	<i>Staphylococcus aureus</i>	0,732
	6	<i>Staphylococcus aureus</i>	0,177

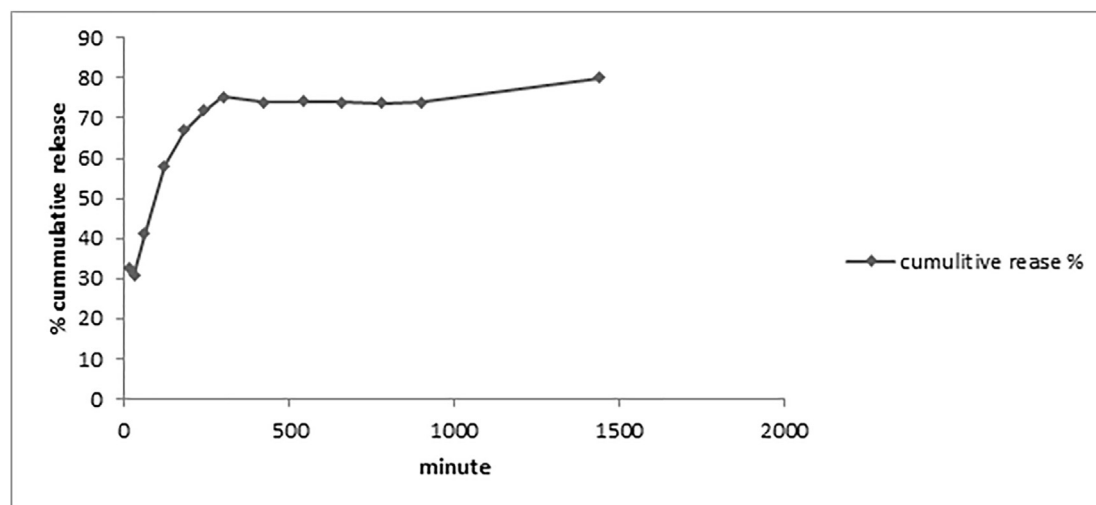


Fig. 5. 1–1440 min's cumulative percent release in pH 7.4.

antibacterial effect, particularly films with a 70% (BNC/Ch) - 30% TQ ratio, against *Salmonella typhimurium* bacteria. This heightened effect is likely attributed to the TQ ratio in the basal source. The antibacterial properties of the films obtained with these ratios are deemed sufficient and suitable for use as drug coating material. Additionally, SEM and FTIR analyses revealed that an increase in the BNC ratio resulted in surface openings in the film, leading to the separation of highly volatile TQ. This observation suggests that selecting a 70% (BNC/Ch) - 30% TQ ratio for film coating would be more effective in terms of antibacterial properties and practical usage.

3.4. Result of release test

The equation of the graph, which is formed by the change of the absorbance values measured for the calculation of the cumulative emission, is as follows.

$$y = 0,0058 \ln(x) + 0,0018 \quad [1]$$

$$R^2 = 0,8435$$

Fig. 5 demonstrates the release profile of BSA, indicating two distinct stages based on the release rate. Initially, there was a rapid release of BSA from the BNC/Ch composite, characterized by a burst release of up to 32% within the first 30 min. Over the subsequent 5 h, this release continued, reaching approximately 76%. In the second stage, the release further increased to 80% over the course of the 24-h measurement period.

4. Conclusions

In summary, we present the development and synthesis of a controlled and sustained-release nano delivery platform using BNC/Ch with various coating agents. FTIR analysis confirmed the presence of functional groups from the coating agents and drug conjugates, indicating successful coating. This was further supported by FESEM surface morphology analysis. *In vitro* drug release studies under simulated human body conditions (pH 7.4) suggested that the drug release profiles followed a pseudo-second order kinetic model. Incorporating surface coating agents hinted at the potential for reducing dosing frequency while extending TQ's efficacy due to sustained-release characteristics. BNC/Ch-TQ composite films, particularly those with a 70% (BNC/Ch) - 30% TQ ratio, exhibited the highest antibacterial effect against *Salmonella typhimurium* bacteria. This effect is attributed to the TQ ratio in the composite. The antibacterial properties of films at these ratios are deemed sufficient for use as drug coating material, with the 70% (BNC/Ch) - 30% TQ ratio being particularly effective. BNC/Ch-TQ composites hold promise for controlled drug delivery coatings and antibacterial wound dressings.

Funding

There is no fund provider.

Conflict of interest

There is no conflict of interest.

References

- [1] Amin MCIM, Abadi AG, Ahmad N, Katas H, Jamal JA. Bacterial cellulose film coating as drug delivery system:

- physicochemical, thermal and drug release properties. *Sains Malays* 2012;41:561–8.
- [2] Dev A, Binulal NS, Anitha A, Nair SV, Furuike T, Tamura H, et al. Preparation of poly(lactic acid)/chitosan nanoparticles for anti-HIV drug delivery applications. *Carbohydrate Polym* 2010;80:833–8. <https://doi.org/10.1016/j.carbpol.2009.12.040>.
 - [3] Cuppok Y, Muschert S, Marucci M, Hjaertstam J, Siepmann F, Axelsson A, et al. Drug release mechanisms from Kollicoat SR:Eudragit NE coated pellets. *Int J Pharm* 2011;409:30–7. <https://doi.org/10.1016/j.ijpharm.02.026>.
 - [4] Maniruzzaman M, Boateng JS, Snowden MJ, Douroumis D. A review of hot-melt extrusion: process technology to pharmaceutical products. *ISRN Pharmaceutics* 2012:e436763. <https://doi.org/10.5402/2012/436763>.
 - [5] Barbu E, Verestiuc L, Nevell TG, Tsibouklis J. Polymeric materials for ophthalmic drug delivery: trends and perspectives. *J Mater Chem* 2016;16:3439–43. <https://doi.org/10.1039/B605640G>.
 - [6] Achouri D, Alhanout K, Piccerelle P, Andrieu V. Recent advances in ocular drug delivery. *Drug Dev Ind Pharm* 2013;39:1599–617. <https://doi.org/10.3109/03639045.2012.736515>.
 - [7] Hearnden V, Sankar V, Hull K, Juras DV, Greenberg M, Kerr AR, et al. New developments and opportunities in oral mucosal drug delivery for local and systemic disease. *Adv Drug Deliv Rev* 2012;64:16–28. <https://doi.org/10.1016/j.addr.2011.02.008>.
 - [8] Janßen EM, Schliephacke R, Breitenbach A, Breikreutz J. Drug-printing by flexographic printing technology—a new manufacturing process for orodispersible films. *Int J Pharm* 2013;441:818–25. <https://doi.org/10.1016/j.ijpharm.2012.12.023>.
 - [9] Morales JO, McConville JT. Manufacture and characterization of mucoadhesive buccal films. *Eur J Pharm Biopharm* 2011;77:187–99. <https://doi.org/10.1016/j.ejpb.2010.11.023>.
 - [10] Nair AB, Kumria R, Harsha S, Attimarad M, Al-Dhubiab BE, Alhaider IA. In vitro techniques to evaluate buccal films. *J Contr Release* 2013;166:10–21. <https://doi.org/10.1016/j.jconrel.2012.11.019>.
 - [11] Al-Kassas R, Seyfoddin A. Biodegradable polymers for controlled delivery of bioactive macromolecules. Nova publisher; 2011. <https://researchspace.auckland.ac.nz/handle/2292/11920>.
 - [12] Shukla SK, Mishra AK, Arotiba OA, Mamba BB. Chitosan-based nanomaterials: a state-of-the-art review. *Int J Biol Macromol* 2013;59:46–58. <https://doi.org/10.1016/j.ijbiomac.2013.04.043>.
 - [13] Azad AK, Sermsintham N, Chandkrachang S, Stevens WF. Chitosan membrane as a wound-healing dressing: characterization and clinical application. *J Biomed Mater Res B Appl Biomater* 2004;69B:216–22. <https://doi.org/10.1002/jbm.b.30000>.
 - [14] Cai S, Liu Y, Zheng Shu X, Prestwich GD. Injectable glycosaminoglycan hydrogels for controlled release of human basic fibroblast growth factor. *Biomaterials* 2005;26:6054–67. <https://doi.org/10.1016/j.biomaterials.2005.03.012>.
 - [15] Zhang P, Chen L, Zhang Q, Hong FF. Using in situ dynamic cultures to rapidly biofabricate fabric-reinforced composites of chitosan/bacterial nanocellulose for antibacterial wound dressings. *Front Microbiol* 2016;7. <https://doi.org/10.3389/fmicb.2016.00260>.
 - [16] Uchegbu IF, Carlos M, McKay C, Hou X, Schätzlein AG. Chitosan amphiphiles provide new drug delivery opportunities. *Polym Int* 2014;63:1145–53. <https://doi.org/10.1002/pi.4721>.
 - [17] Liu M, Zhou Y, Zhang Y, Yu C, Cao S. Preparation and structural analysis of chitosan films with and without sorbitol. *Food Hydrocoll* 2013;33:186–91. <https://doi.org/10.1016/j.foodhyd.2013.03.003>.
 - [18] Shah N, Ul-Islam M, Khattak WA, Park JK. Overview of bacterial cellulose composites: a multipurpose advanced material. *Carbohydr Polym* 2013;98:1585–98. <https://doi.org/10.1016/j.carbpol.2013.08.018>.
 - [19] Czaja WK, Young DJ, Kawecki M, Brown RM. The future prospects of microbial cellulose in biomedical applications. *Biomacromolecules* 2007;8:1–12. <https://doi.org/10.1021/bm060620d>.
 - [20] Hu W, Chen S, Li X, Shi S, Shen W, Zhang X, et al. In situ synthesis of silver chloride nanoparticles into bacterial cellulose membranes. *Mater Sci Eng* 2009;C 29:1216–9. <https://doi.org/10.1016/j.msec.2008.09.017>.
 - [21] Wan YZ, Luo H, He F, Liang H, Huang Y, Li XL. Mechanical, moisture absorption, and biodegradation behaviours of bacterial cellulose fibre-reinforced starch biocomposites. *Compos Sci Technol* 2009;69:1212–7. <https://doi.org/10.1016/j.compscitech.2009.02.024>.
 - [22] Trovatti E, Freire CSR, Pinto PC, Almeida IF, Costa P, Silvestre AJD, et al. Bacterial cellulose membranes applied in topical and transdermal delivery of lidocaine hydrochloride and ibuprofen: in vitro diffusion studies. *Int J Pharm* 2012;435:83–7. <https://doi.org/10.1016/j.ijpharm.2012.01.002>.
 - [23] Javidi S, Razavi BM, Hosseinzadeh H. A review of neuropharmacology effects of *Nigella sativa* and its main component, thymoquinone. *Phytother Res* 2016;30:1219–29. <https://doi.org/10.1002/ptr.5634>.
 - [24] Schneider-Stock R, Fakhoury IH, Zaki AM, El-Baba CO, Gali-Muhtasib HU. Thymoquinone: fifty years of success in the battle against cancer models. *Drug Discov Today* 2014;19:18–30. <https://doi.org/10.1016/j.drudis.2013.08.021>.
 - [25] Banerjee S, Padhye S, Azmi A, Wang Z, Philip PA, Kucuk O, et al. Review on molecular and therapeutic potential of thymoquinone in cancer. *Nutr Cancer* 2010;62:938–46. <https://doi.org/10.1080/01635581.2010.509832>.
 - [26] Mendes RG, Bachmatuik A, Büchner B, Cuniberti G, Rummeli MH. Carbon nanostructures as multi-functional drug delivery platforms. *J Mater Chem* 2012;B 1:401–28. <https://doi.org/10.1039/C2TB00085G>.
 - [27] Patra JK, Das G, Fraceto LF, Campos EVR, Rodriguez-Torres M, del P, et al. Nano based drug delivery systems: recent developments and future prospects. *J Nanobiotechnol* 2018;16:71. <https://doi.org/10.1186/s12951-018-0392-8>.
 - [28] Zangabad PS, Karimi M, Mehdizadeh F, Malekzad H, Ghasemi A, Bahrami S, et al. Nanocaged platforms: modification, drug delivery and nanotoxicity, Opening synthetic cages to release the tiger. *Nanoscale* 2017;9:1356–92. <https://doi.org/10.1039/C6NR07315H>.
 - [29] Gursoy C, Sofu A, Ekinci FY. Cellulose production potential of lactic acid bacteria. Süleyman Demirel University, Isparta; Yeditepe University, Istanbul, Turkiye. *Nanomed & Nanobiotech*; 2015.
 - [30] Fajardo P, Martins JT, Fuciños C, Pastrana L, Teixeira JA, Vicente AA. Evaluation of a chitosan-based edible film as carrier of natamycin to improve the storability of Saloio cheese. *J Food Eng* 2010;101:349–56. <https://doi.org/10.1016/j.jfoodeng.2010.06.029>.
 - [31] Kim J, Cai Z, Lee HS, Choi GS, Lee DH, Jo C. Preparation and characterization of a Bacterial cellulose/Chitosan composite for potential biomedical application. *J Polym Res* 2011;18:739–44. <https://doi.org/10.1007/s10965-010-9470-9>.
 - [32] Ostadhosseini F, Mahmoudi N, Morales-Cid G, Tamjid E, Navas-Martos FJ, Soriano-Cuadrado B, et al. Development of chitosan/bacterial cellulose composite films containing nanodiamonds as a potential flexible platform for wound dressing. *Materials* 2015;8:6401–18. <https://doi.org/10.3390/ma8095309>.
 - [33] Türkyilmaz S, Sava S, Kaya O. Tavuklarda Salmonella enteritidis infeksiyonlarının bakteriyolojik ve Serolojik yöntemlerle Teşhisi. *J Fac Vet Med Istanbul Univ* 2007;33:23–33. <https://doi.org/10.16988/iuvfd.65173>.
 - [34] Pagola S, Benavente A, Raschi A, Romano E, Molina MAA, Stephens PW. Crystal structure determination of thymoquinone by high-resolution X-ray powder diffraction. *AAPS PharmSciTech* 2004;5:24–31. <https://doi.org/10.1208/pt050228>.
 - [35] Kuçukoğuz AO, Uslu MK. Cooking loss, tenderness, and sensory evaluation of chicken meat roasted after wrapping with edible films. *Food Sci Technol Int* 2018. <https://doi.org/10.1177/1082013218776540>.
 - [36] Sun T, Wu C, Hao H, Dai Y, Li J. Preparation and preservation properties of the chitosan coatings modified with the in situ synthesized nano SiO_x. *Food Hydrocoll* 2016;54:130–8. <https://doi.org/10.1016/j.foodhyd.2015.09.019>.